

5. TEST AND MATERIALS STANDARDS

A. Rolling Contact Fatigue

Andrew A. Wereszczak
Ceramic Science and Technology Group (CerSaT)
Oak Ridge National Laboratory
PO Box 2008, MS 6068
Oak Ridge, TN 37831-6068
(865) 576-1169; fax: (865) 574-6098; e-mail: wereszczakaa@ornl.gov

DOE Technology Development Area Specialist: James J. Eberhardt
(202) 586-9837; fax: (202) 586-1600; e-mail: james.eberhardt@ee.doe.gov
Field Technical Manager: D. Ray Johnson
(865) 576-6832; fax: (865) 574-6098; e-mail: johnsondr@ornl.gov

Contractor: Oak Ridge National Laboratory, Oak Ridge, Tennessee
Prime DOE Contract Number: DE-AC05-00OR22725

Objectives

- Enable greater use of next-generation ceramic and coated-metal roller elements for diesel engines through rolling contact fatigue (RCF) and microstructural characterizations.
- Link surface and subsurface flaws to RCF response to enable microstructural engineering that will promote microstructure engineering and improved RCF performance.
- Link RCF performances measured by different internationally used RCF test techniques.

Approach

- Establish three-ball-on-rod (3BOR) RCF test facilities and collaborations with domestic and international institutions that employ different RCF test techniques and correlate test results.
- Vary machining-induced subsurface damage in a Si_3N_4 and correlate that to measured RCF performance and model hypothetical microstructures that will promote improved RCF performance.
- Develop supporting mechanical test methods that enable the study of surface and subsurface flaws in roller elements.

Accomplishments

- Established 3BOR RCF test facility at Oak Ridge National Laboratory.
- Completed summary report on RCF test methods and result interpretations used in Germany, Japan, United Kingdom, and the United States.
- Developed method to evaluate and discriminate the elastic properties of ball bearings in situ using resonance ultrasound spectroscopy (RUS).
- Conceived “c-sphere” flexure strength specimen to enable surface flaw examination.

Future Direction

- Conduct International interlaboratory study to compare 3BOR performances of a selected Si_3N_4 .
- Compare RCF damage on rods and balls of a selected Si_3N_4 with the same coarse and fine grinding.
- Refine the geometry and testing of the “c-sphere” flexure strength specimen and the ability to characterize surface and subsurface damage in finished ceramic balls and link to RCF performance.
- Link surface and subsurface flaws to RCF performance.

Introduction

Technical ceramics used as materials for rolling contact bearing components show several practical advantages over traditional bearing steels. The properties of ceramics, specifically low density, high stiffness, high hardness, low coefficient of thermal expansion, and high-temperature capability are properties suited to rolling element materials. Silicon nitride (Si_3N_4) has been found to have a good combination of properties suitable for these applications. Research over the past three decades on structure, quality control, and manufacturing techniques has produced ceramic materials that are suitable alternatives to steel for rolling contact bearing design. This is especially true for hybrid ball bearings (i.e., precision angular contact ball bearings using ceramic rolling elements) that are now offered as standard components within the ball bearing manufacturing industry.

An expansion in the use of ceramic bearings necessitates guidelines for the choice of bearings or rolling elements. In light of these requirements, ASTM standard F2094-01, “Standard Specification of Silicon Nitride Bearing Balls,” has been issued recently. The dimensional specifications of balls are based on those of rolling element bearing steel balls. The most remarkable thing in the standard is that the ranking of Si_3N_4 's mechanical properties is provided depending on various applications of bearings. However, nothing is described about rolling contact fatigue (RCF) behavior, which is fundamental information to assess the lifetime of the material. Due to the lack of such information, some concern for the reliability of ceramic bearings still remains.

RCF is the surface damage process due to the repeated application of stresses when the surfaces of two bodies roll on each other. RCF is encountered most often in rolling element bearings and gears. The failure process of RCF involves fatigue crack initiation and propagation, which is related to the

characteristics of the surface and subsurface quality or flaw population, stress distributions, and lubrication condition. Presently, surface crack defects are considered as a main factor that causes RCF failure. It is difficult to detect these surface cracks during high-volume production processes, and hence it is crucially important to understand their influence and the fundamental mechanism of the failures they cause.

To address these issues, this project characterizes the RCF performance of Si_3N_4 compositions that are under consideration for use, or that are presently used, in rolling element components (e.g., hybrid bearings—see Figure 1, cam roller followers, etc.). The study of the effects that subsurface damage and the stress state from Hertzian contact have on RCF performance is a primary component to this project. Several different test methods are used internationally to measure RCF performance, so this project also works toward reconciling their

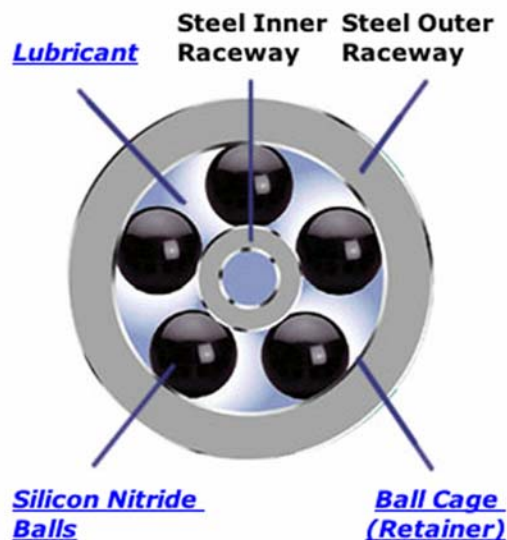


Figure 1. Schematic of a hybrid bearing system that includes silicon nitride balls. Image from Cerbec Web site (www.cerbec.com).

measured differences so that their results can be validly pooled. Based on all these findings, hypothetical microstructures that will promote improved RCF performance will be identified and shared with ceramic manufacturers.

Approach

There are three primary aspects to the project: (1) examine the effects that subsurface damage and microstructure have on RCF performance, (2) measure RCF performance and reconcile results that were generated using different RCF test techniques, and (3) iteratively work with ceramic manufacturers and communicate RCF results and interpretations that those manufacturers can then use to develop lower cost Si_3N_4 compositions or improve Si_3N_4 machinability or improve RCF performance or combinations thereof.

Results

Effects of Surface and Subsurface Damage

The “C-Sphere” flexure strength specimen was conceived and preliminarily developed to measure the strength of bearing-grade Si_3N_4 balls and to relate that property to surface-located strength-limiting flaws (e.g., machining damage) *and to ultimately link those flaw populations to RCF performance*. A slot is machined into the balls to a set depth to produce the “C-sphere” geometry. C-sphere specimens are then diametrically compressed to produce a monotonically increasing hoop tensile stress at their surface that ultimately caused their fracture (see Figure 2). Strength is determined using the combination of failure load, C-sphere geometry, and FEA.

The stress field was used to determine C-sphere effective areas and effective volumes as a function of Weibull modulus. A quarter symmetry model for the C-sphere specimen is shown in Figure 3 with the mesh distribution that was ultimately used to evaluate its effective volume and area. Solid95 tetrahedral elements were used, and a 100-N point load was applied to the sphere’s apex. The mesh contained 52703 elements and 76682 nodes. As can be seen from Figure 3, finer mesh density was used in the region where high tensile stresses would develop, gradually getting coarser toward the area where the load is applied and the overhang section. The ball from which the specimen was simulated had the

dimensions of a 12.7-mm diameter and a slot width of 6.35 mm.

The issue of artificially high stress concentration within the narrow zone under the applied point load and its effect on the computed effective sizes was considered. In the virtual world of finite element analysis (FEA), the load is applied as a perfectly concentrated point load, which causes stress singularity in that region. This is an idealization of what physically takes place where distributed load acting over a narrow area is actually applied. In other words, as the mesh gets finer, the stress under the load will increase indefinitely making the model and hence the effective sizes mesh dependent.

To understand the issue of stress singularity under the point load, both nodal and element first principal stress distributions are shown in Figures 4 and 5 for the intermediate and fine mesh models, respectively. A nodal plot smooths the stress distribution by averaging the stresses at that point in all the elements having that common node. This smoothing is masking the very high stresses taking place within the individual elements, which if not removed would yield erroneous effective size calculations. This is because when the effective size is computed, the stress distribution is normalized with respect to the maximum effective stress in the component. If this maximum effective stress were incorrect, due for example, to a localized stress concentration, as is the case for this model, then the computed value would be incorrect. To unmask the

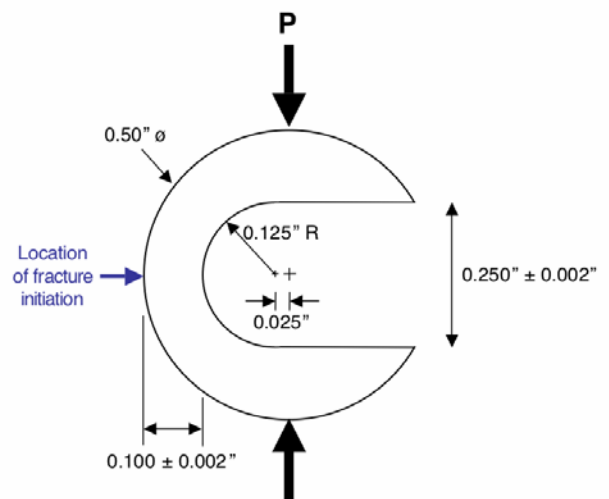


Figure 2. Schematic of the “C-Sphere” test specimen and its diametral compressive loading. Fracture will initiate at the outer surface and propagate radially inward.

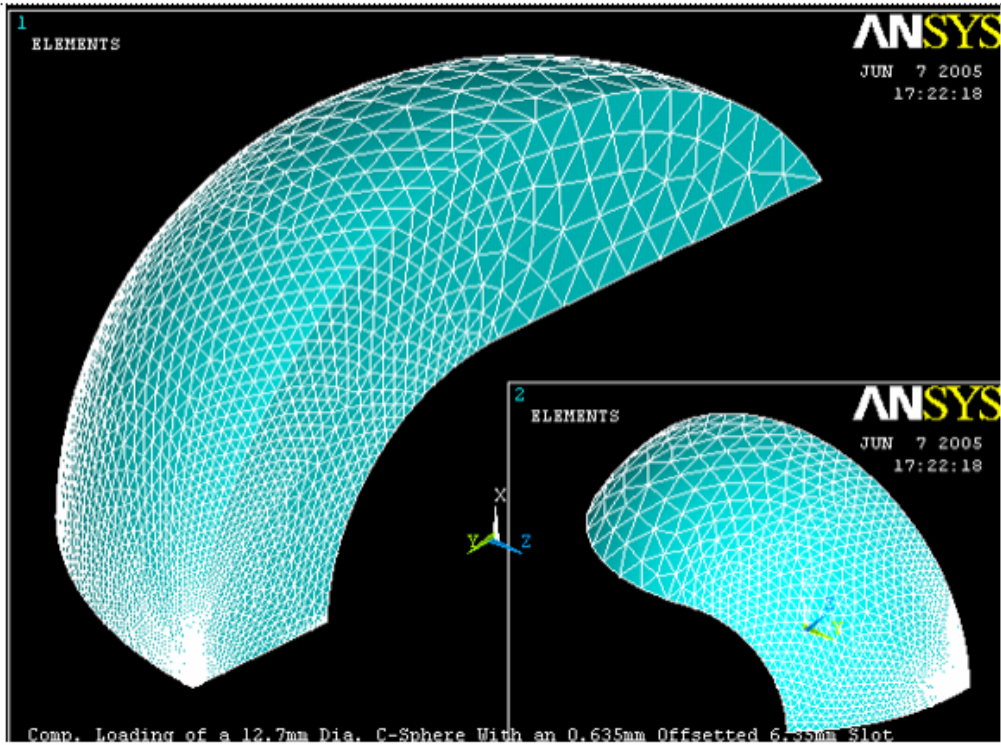


Figure 3. Mesh distribution for one-fourth symmetry model of the C-sphere specimen, having 52703 elements and 76682 nodes. Three different mesh densities were used to evaluate the specimen, and they were coarse (8497 elements), intermediate (16090 elements), and fine mesh (shown—52703 elements).

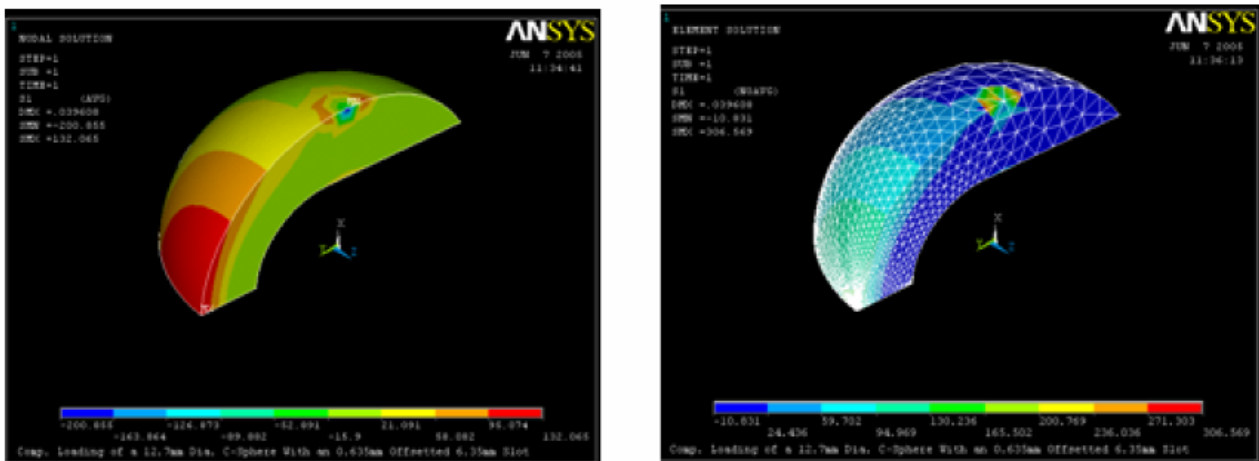


Figure 4. Nodal first principal stress distribution (left) and element first principal stress distribution (right) for the C-sphere specimen, using the intermediate mesh model.

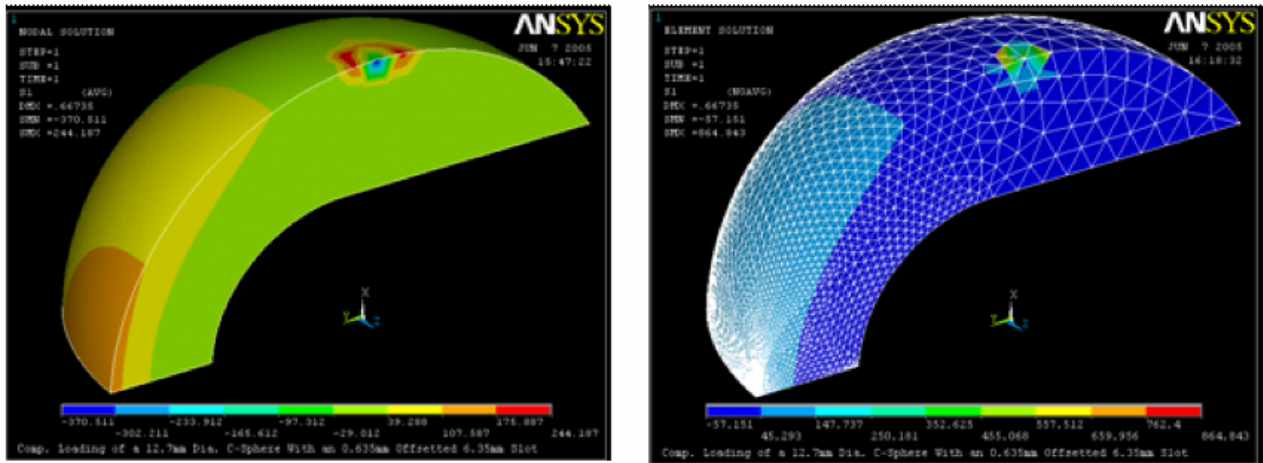


Figure 5. Nodal first principal stress distribution (left) and element first principal stress distribution (right) for the C-sphere specimen, using the fine mesh model.

high nodal stresses, element stress plots are used that display the actual nodal stresses as computed for each element.

The nodal and element first principal stress distributions for the C-sphere specimen using the intermediate mesh model are shown in Figure 4. As can be seen from the nodal plot, the maximum tensile stress is computed to be 132.1 MPa, taking place at the side of the sphere as expected. However, when the element stress plot is examined, the high tensile stress (306-MPa) region shifts to the area under the load, which is obviously an artifact of the point load effect. For the fine mesh model (Figure 5), both nodal and element stress plots show the highest tensile stress region to be under the point load, with the maximum first principal nodal and element stresses increasing to 244 MPa, and 644 MPa, respectively. Figures 4 and 5 clearly show that the stresses under the load are extremely mesh dependent and will keep changing as the mesh changes; for the rest of the specimen, the stresses have long converged even for the coarse mesh specimen model.

To take out the effect of localized stress concentration on the effective size calculations, the artificially high stressed elements under the load were removed. The remaining elements, comprising the vast majority of the specimen, were then used to assess the specimen’s effective sizes. The nodal and element stress distribution plots for the C-sphere model are shown in Figure 6, with the highly stressed elements carved out. One would then observe from these plots how the maximum tensile

stress of 132 MPa shifts back to the side of the specimen where it should be. The fact that both the nodal and element stress plots yield the same stress distribution indicates that the suspect elements were successfully removed and that the remaining model can now be used to compute the effective sizes. Hence, it is the model in Figure 6 that was utilized to compute the effective area and effective volume for the C-sphere specimen.

The effective area (A_e) and effective volume (V_e) as function of Weibull modulus for the C-sphere specimen are illustrated in Figures 7–8, respectively. The effective sizes were computed using the following equations:

$$A_e = \left(\frac{\sigma_0}{\sigma_e} \right)^m \ln \left(\frac{1}{1 - P_f} \right),$$

$$V_e = \left(\frac{\sigma_0}{\sigma_e} \right)^m \ln \left(\frac{1}{1 - P_f} \right),$$

where σ_0 is the scale parameter, m is the Weibull modulus, σ_e is the maximum effective stress (computed by CARES/Life), and P_f is the probability of failure (computed by CARES/Life). The effective sizes are independent of the scale parameter because they only vary with geometry, loading, and the Weibull modulus. Hence, the scale parameter was assigned a random value in order to carry out the reliability and effective size calculations.

To achieve familiarity with the new C-sphere geometry, approximately 30 finished Si_3N_4 spheres

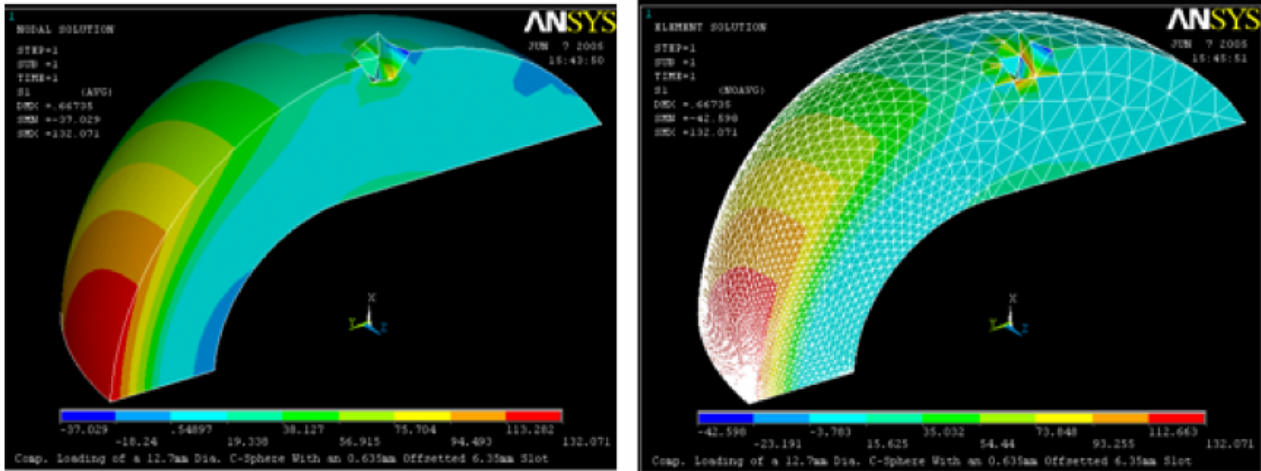


Figure 6. Nodal first principal stress distribution (left) and element first principal stress distribution (right) for the C-sphere specimen using the fine mesh model with the elements within the high stress concentration zone (under the load) carved out. This is the model used to evaluate the effective sizes whose results are shown in Figures 7–8.

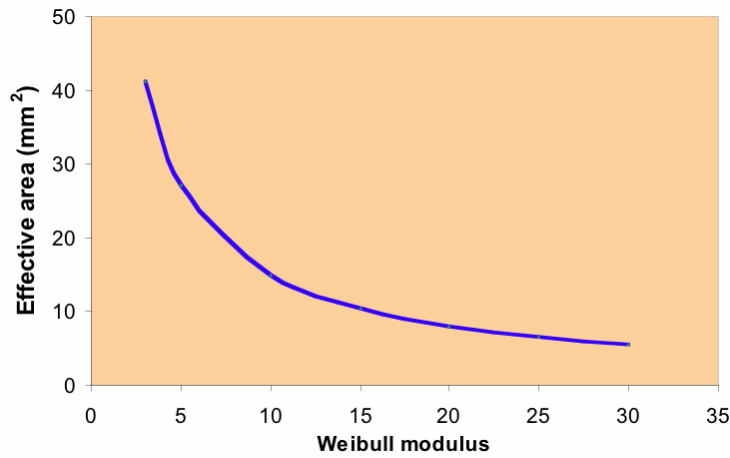


Figure 7. Effective area vs Weibull module for the C-sphere specimen.

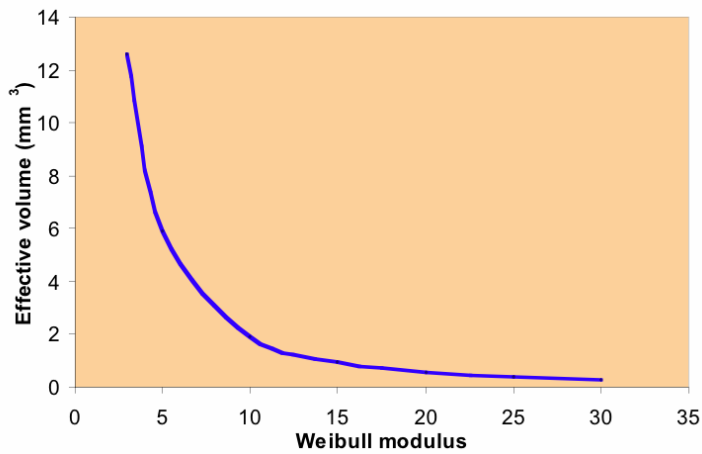


Figure 8. Effective volume vs Weibull module for the C-sphere specimen.

were machined according to Figure 2 and were strength tested. The failure loads and geometrical parameters are now being combined to calculate strength and for interpretation. Additional C-sphere specimens of NBD200, SN101C, and TSN-03NH will be machined to generate more confident Weibull statistics, and C-sphere tests from balls machined according to Table 1 will be performed too. Fractography will then be performed to link strength-limiting flaw type to strength and ultimately RCF performance.

All four machined ball sets have been received (see Table 1). Bournemouth University is using the one larger diameter set to reduce to a 12.7-mm diameter using an internally developed lapping procedure that will essentially yield a fourth (lapped) finish condition.

The utility of using resonant ultrasound spectroscopy (RUS) to quantify elastic properties of Si₃N₄ balls, to assess consistency of those properties, and (hopefully) be able to nondestructively proof test them or identify preexisting flaws is under exploration. H. Trivedi of UES (an Air Force Research Laboratory contractor) forwarded numerous Si₃N₄ balls that were damaged from their RCF testing for attempted RUS characterization and that is under way. Part of those supplied balls included pristine Toshiba TSN-03NH balls whose elastic properties were measured with the RUS and compared with those of NBD 200 and SN101C silicon nitrides. Their comparison is shown in Figure 9, and it was observed that the TSN-03NH balls showed the least amount of variability in those properties of the three Si₃N₄ compositions. The elastic properties

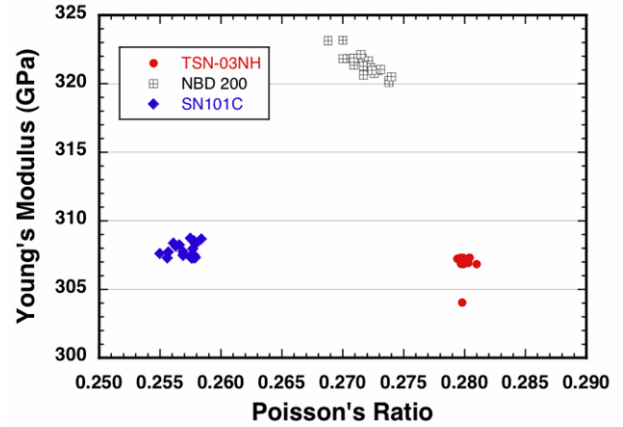


Figure 9. Elastic modulus and Poisson’s ratio distributions for three bearing grade Si₃N₄ materials as measured with RUS.

of the three 12.7-mm-diameter sets listed in Table 1 were also measured with RUS, and those results are shown in Figure 10. Several of the balls showed variability, but it may be argued that close clustering of data suggest that most of the ball diameters and material density were uniform and that machining condition did not affect that.

To better understand RCF damage and its link to material microstructure, several supplemental characterization test methods are used. For example, instrumented static and dynamic indentation testing, and instrumented scratch testing of the Ceralloy 147-31N is used to explore how contact loading damage (as a function of loading rate) is affected by subsurface damage. The competition of quasi-plastic damage and cracking processes in Ceralloy 147-31N

Table 1. Grinding conditions for silicon nitride spheres

Step	Diameter & finish	Wheel	Removal (in.)	Removal per pass (in.)
12.7 mm/0.500 in. Coarse	1 (roughing)	Accepted practice		0.001
	2 (induce damage)	100 grit	0.004	0.001
	3 (finishing)	600 grit	0.0005	0.0001
13.2 mm/0.520 in. Coarse	1 (roughing)	Accepted practice		0.001
	2 (induce damage)	100 grit	0.004	0.001
	3 (finishing)	600 grit	0.0005	0.0001
12.7 mm/0.500 in. Fine	1 (roughing)	Accepted practice		0.001
	2 (induce damage)	180 grit	0.004	0.001
	3 (finishing)	600 grit	0.0005	0.0001
12.7 mm/0.500 in. RCF-conventional	“Accepted” practice for RCF test bar finishing			

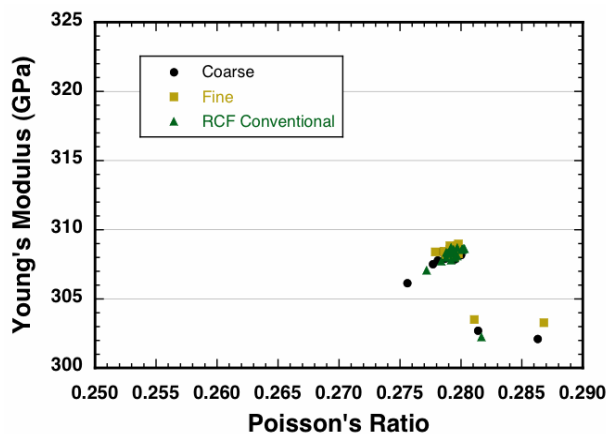


Figure 10. Elastic modulus and Poisson's ratio distributions for Ceralloy 147-31N Si_3N_4 balls as measured with RUS. The three sets were machined per the conditions in Table 1.

is being interrogated as a function of the depth of the subsurface damage and compared to polished material as well. NBD200 Si_3N_4 (NIST SRM for Knoop hardness) and NC132 Si_3N_4 (NIST SRM for fracture toughness) are also being tested; specimens of those materials are presently undergoing indentation and scratch testings whose results will serve as a performance reference for comparisons of performances of Ceralloy 147-31N and whatever additional ceramics that are ultimately tested in this program. SN101C and TSN-03NH (both bearing grades of Si_3N_4) are undergoing instrumented indentation and scratch testings as well, and their performances will be compared with those of the other listed silicon nitride compositions. Raman spectroscopy, and its ability to measure residual stresses, is being used. Preliminary results suggest that residual stresses (manifested by changes in wave number peak location in Figure 8) can indeed be quantified.

Reconciliation of RCF Test Results

A summary report was completed that describes RCF test methods used in Germany, Japan, United Kingdom, and the United States and the interpretation of their results. The report will be published as an ORNL Technical Report.

Japan's National Institute of Advanced Industrial Science and Technology (AIST) will start a 3-year standardization project of RCF testing funded by Japan's Ministry of Economy, Trade, and Industry (METI), Japan, in Quarter 4, and the pre-

sent project will collaborate. AIST's W. Kanematsu invited this project participation for the purpose of performing three-ball-on-rod (3BOR) RCF testing. The UK National Physical Laboratory (NPL) and Germany (BAM) will also participate. AIST will provide materials for the testing.

Interaction with Domestic Manufacturers

Dialog with ceramic bearing manufacturers is critical to relevance being maintained in this program. Frequent communication occurs between the principal investigator and chief scientists at several domestic manufacturers (Cerbec/Saint-Gobain, Ceradyne, Encerateg, Kennametal, and Cercom) regarding this project's test matrix, plans, and progress.

Conclusions

A 3BOR RCF test facility was established in ORNL, and the evaluation of ceramic RCF performance of Si_3N_4 roller element materials is now well under way. A formal collaboration is under way with BU for three ball-on-ball (3BOB) RCF testing of ceramics, and this enables the eventual reconciliation of RCF performances measured with those two techniques. The effects of subsurface damage on RCF performance are being scrutinized with the C-sphere flexure strength specimen. A summary report was completed that describes RCF testing and result interpretations used in Germany, Japan, the United Kingdom, and the United States. A method was developed to evaluate and discriminate the elastic properties of ball bearings in situ using resonance ultrasound spectroscopy. Ultimately, the results from this project will link surface and subsurface flaws to RCF performance and enable greater use of next-generation ceramic and coated-metal roller elements for diesel engines through RCF and microstructural characterizations.

Presentations and Publications

A. A. Wereszczak, W. Wang, O. M. Jadaan, and M. J. Lance, "Strength of a C-Sphere Specimen," abstract submitted to the January 2006 Cocoa Beach conference.

Y. Wang, M. Hadfield, W. Wang, and A. A. Wereszczak, "Rolling Contact Fatigue of Ceramics," in internal review, to be published as a DOE/ORNL Technical Memorandum.